Sensors & Actuators: B. Chemical 321 (2020) 128608

Contents lists available at ScienceDirect

Sensors and Actuators B: Chemical

journal homepage: www.elsevier.com/locate/snb

Metal-organic framework portable chemical sensor

Chen Zhu, Rex E. Gerald II, Yizheng Chen, Jie Huang*

Department of Electrical and Computer Engineering, Missouri University of Science and Technology, Rolla, MO, 65409, USA

ARTICLE INFO

Keywords:
Chemical sensor
Metal-organic framework
Coaxial cable sensor
Open-ended coaxial cable resonator
Enhanced sensitivity
Microwave resonator
Carbon dioxide
Methane
HKUST-1

ABSTRACT

Combining the chemical-specific adsorption properties of metal-organic framework (MOF) materials with the dielectric sensitivity of a novel open-ended hollow coaxial cable resonator (OE-HCCR), a mechanically-robust and portable gas sensor device (OE-HCCR-MOF) with high chemical selectivity and sensitivity is proposed and experimentally demonstrated. The operating principle of the device is based on changes in the dielectric property of the host MOF layer in response to variations in the types and concentrations of guest molecules. The changes in the dielectric property of the MOF layer modify the phase-matching condition of the microwave resonator, causing shifts in the resonance frequency of the device. By monitoring the resonance frequency shift, the adsorptions of guest molecules can be monitored in real-time and accurately quantified. In proof-of-concept demonstrations, a 200-μm layer of MOF (HKUST-1) was placed within an OE-HCCR to develop a prototype OE-HCCR-MOF sensor. The novel sensor showed high sensitivity to variations in the concentrations of carbon dioxide with good reversibility. The chemical selectivity of the prototype sensor for carbon dioxide compared to methane was also investigated.

1. Introduction

Sensing common gases and volatile organic compounds (VOCs) with high sensitivity and selectivity is of significant importance for monitoring environmental pollutants, controlling greenhouse gas emissions, and homeland security needs (e.g., detection of harmful or dangerous target analytes at airport check-points) [1]. Gas chromatography-mass spectroscopy (GC–MS) is an effective tool for separating, identifying, and quantifying complex mixtures of gas analytes. However, the utilization of GC–MS methods involves cumbersome instrumentation, troublesome sample condensation, and sophisticated method development [2]. Therefore, innovations that advance reliable, portable, and cost-effective sensors for *in situ* and real-time monitoring of gaseous targets are highly desirable. Nanoporous material-assisted portable sensing devices have gained broad research interest in the past decade. These devices operate based on measurements of changes in the physical/chemical properties of the nanoporous material due to selective chemical interactions or physical adsorption of the target analyte. The high surface-to-volume ratio and high porosity of nanoporous materials enable efficient inclusion of gaseous target analytes inside host materials and thereby drastically improve the measurement sensitivity and facilitates the detection of target analytes down to lower limits [3–6]. One of the most popular and well-established nanoporous materials that have been continuously explored for this application is the zeolite family, a microporous aluminosilicate crystalline material with nanometer-scale or angstrom-scale pore systems [7,8], which is chemically and thermally stable in harsh-environments. However, zeolite materials present a rather limited variety of chemical functionalities tailored for adsorption of chemical species due to the challenges of fine-tuning specific pore sizes and chiral channels [9].

Metal-organic frameworks (MOFs) are a newer category of crystalline nanoporous materials that have been extensively investigated recently in the areas of storage of greenhouse gases, gas separation, catalysis, and removal of impurities in natural gas [10–12]. MOFs are formed by the coordination of metal cations and organic linkers. The variety of metal ions, organic linkers, and how the metal ions are joined with the organic linkers provide MOFs with unparalleled design features compared to other classes of nanoporous materials. These design features include a high degree of tunability, structural diversity, and tailorable chemical and physical properties. The possibilities of employing MOFs for sensing applications were only explored recently [1]. Particularly, the tailorable chemical selectivity, as well as high mechanical, thermal, and chemical stability make MOFs appealing to researchers in the fields of chemical sensing and instrumentation.

Optical fibers and coaxial cables are the two most widely used transmission lines in telecommunications for transmitting signals over long distances. Apart from communication applications, the two waveguides have also been investigated as platforms for various sensing

* Corresponding author.
E-mail address: jieh@mst.edu (J. Huang).

https://doi.org/10.1016/j.snb.2020.128608
Received 30 April 2020; Received in revised form 4 July 2020; Accepted 16 July 2020
Available online 17 July 2020

purposes, i.e., fiber-optic sensors and coaxial-cable sensors. The surge in popularity of these sensor devices came about because they offer unique features such as high sensitivity, harsh-environment survivability, remote operation, and capability for multiplexing [13–16]. Examples include refractometers for measurements of the dielectric property of an analyte, i.e., fiber-optic refractometers and coaxial-cable devices for dielectric spectroscopy [17–20].

Recent studies revealed that the dielectric properties of MOFs are dependent on the types, amounts, and the states of the molecular guests loaded in the pores of the MOF crystals [21,22]. Loading and unloading guest molecules in host MOF crystals result in changes in permittivity of the host MOF. Therefore, combining the chemical selectivity of MOFs and the high sensitivity of waveguide-based dielectric spectroscopy might provide a solution for *in-situ*, reliable, low-cost, and rapid detection of target chemicals. However, there is currently limited literature on this topic [23–32]. The majority of existing reports focused on developing optical fiber-based MOF sensors, where thin films of MOF were coated on the cleaved end facet of a telecommunication optical fiber [27,28] or the cylindrical outer surface of a microstructured optical fiber [23–26,29–31]. These novel devices are diminutive in size and present prominent sensing performances such as rapid response time (~10 s), low detection limit (~ppm level), and excellent stability and reversibility. The concerning issues of fiber-optic MOF devices include the bonding strength between the MOF thin films and the silica fiber surface, the precise control of the MOF film thickness, the uniformity of the thin films, and the mechanical robustness of the whole sensor head, making mass production and real-world applications of these devices challenging. On the other hand, coaxial-cable sensors, in general, offer much higher mechanical strength and ease of fabrication and thereby provide high potential for mass production [14–16,19,20,33–36]. Open-ended coaxial probes have been extensively investigated, standardized, and commercialized for dielectric spectroscopy at microwave frequencies (i.e., 300 MHz ~ 300 GHz) over the past five decades [18,37–40]. A dielectric material positioned at the open end of a coaxial transmission line perturbs the fringing electric field and thereby modifies the amplitude and phase of the electromagnetic signals reflected by the open end. Consequently, the permittivity of the unknown dielectric material can be resolved by analyzing the complex reflection coefficient that characterizes the open end. However, traditional open-ended coaxial cable probes suffer from low measurement sensitivity and resolution and require complicated data analysis. Therefore, a new sensing scheme is desirable to enhance measurement sensitivity. A new scheme should facilitate the combination of MOFs and coaxial-cable sensors for the development of highly-sensitive portable and powerful analytical devices for chemical sensing.

In this work, we propose and demonstrate a porous metal plate-backed open-ended hollow coaxial cable resonator (OE-HCCR) combined with, for the first time, a crystalline MOF dielectric material (OE-HCCR-MOF) for selective gas sensing with high sensitivity. The porous metal plate serves two purposes: (1) It greatly improves the dependence of the fringing electric field on the dielectric material (e.g., MOF) in front of the open end (i.e., it enhances the measurement sensitivity of dielectric spectroscopy by concentrating the fringing electric field); and, (2) It creates a convenient chamber at the open end of the resonator for containing the dielectric MOF layer. The MOF layer not only enables the chemical selectivity of the device but also serves as an analyte concentrator, due to the high surface-to-volume ratio, which enhances the measurement sensitivity of the OE-HCCR-MOF device. The paper continues by deriving a mathematical model of the novel microwave sensing technique and discusses the sensitivity enhancement capability of the device. Experimental results are then presented, based on a prototype chemically-selective OE-HCCR-MOF device, for quantitative measurements of carbon dioxide (CO_2). Finally, the chemical selectivity of the prototype device is further demonstrated by investigating the device's temporal responses to the competitive adsorption of methane (CH_4) and CO_2.

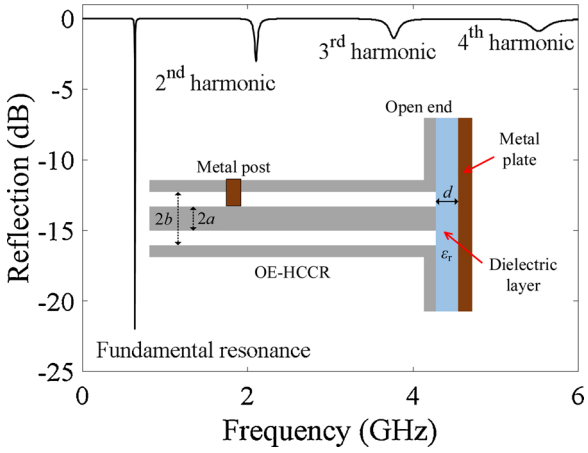

Fig. 1. An overview of the OE-HCCR design and signal output. The graph shows a plot of the calculated reflection spectrum of the OE-HCCR. The inset shows a schematic of the cross-section of the OE-HCCR. The OE-HCCR is terminated by a metal plate-backed dielectric layer. The dielectric layer has a thickness of d and a relative permittivity of ε_r. The diameters of the inner and outer conductors are denoted as $2a$ and $2b$, respectively. For the numerical calculations, the physical parameters of the OE-HCCR were set to the same parameters used to fabricate the prototype device: a = 3.0 mm; b = 7.0 mm; L = 75 mm (the distance between the metal post and the open end of the coaxial cable); and, D = 3.0 mm (diameter of the metal post). The thickness and the relative permittivity of the dielectric layer were set to 0.2 mm and 1, respectively.

2. Methods and materials

2.1. Working principle of OE-HCCR for dielectric measurement

We start by discussing the working principle of the device, the OE-HCCR, for dielectric measurements with high sensitivity. An overview of the OE-HCCR is presented in Fig. 1. The (sensor) resonator output response is plotted in Fig. 1 as a typical frequency-domain reflection spectrum over a 6 GHz bandwidth. The inset in Fig. 1 shows a schematic of the cross-section of the OE-HCCR. Importantly, a conductive metal plate is included in the OE-HCCR as an electric field concentrator and termination plane; the gap between the open end of the coaxial cable and the metal plate is filled with a dielectric layer. The OE-HCCR is designed based on a homemade hollow coaxial cable with air as the dielectric layer for the transmission line. Hollow coaxial cables with air dielectrics have operational advantages at elevated temperatures where conventional dielectrics (e.g., PTFE, PE) are not mechanically and chemically stable for sensing applications in harsh environments. The coaxial cable resonator is formed between two microwave reflectors. A metal post welded within the RF input end shorts the inner conductor and the outer conductor, inducing a large impedance mismatch and serves as the first reflector of the resonator; the open end together with the conductive metal plate-backed dielectric layer serves as the second reflector. Detailed studies of the OE-HCCR can be found in our recent work [41]. Multiple resonance dips can be observed in the resonator output within the observation frequency bandwidth spanning from 10 MHz to 6 GHz, including the fundamental resonance (~0.636 GHz) and higher-order harmonics (i.e., 2nd, 3rd, and 4th harmonics at 2.100 GHz, 3.767 GHz, and 5.519 GHz, respectively). The fundamental resonance dip provides the highest signal-to-noise ratio and is employed as the reference signal for sensing applications. The resonance frequencies (f_{res}) of the OE-HCCR are given by:

$$f_{res} = \frac{c(2m\pi + \phi_1 + \phi_2)}{4\pi L} \quad (1)$$

where c is the speed of light in vacuum; m is a non-negative integer

denoting the resonance order; L is the physical distance between the metal post and the open end; ϕ_1 and ϕ_2 are the phases of the reflection coefficients of the first reflector (i.e., the metal post) and the second reflector (the open end combined with the conductive metal plate-backed dielectric layer), respectively. The fundamental basis for chemical sensing by the OE-HCCR is based on correlating the dielectric property of the layer under test to the resonance frequency (e.g., fundamental resonance frequency). Specifically, the change in permittivity of the dielectric layer modifies the phase reflection coefficient of the open end (ϕ_2), resulting in a change in the resonance frequency of the microwave resonator according to Eq. (1). By monitoring shifts of the fundamental resonance frequency, variations of the permittivity of the dielectric layer can be determined. The conductive metal plate further enhances the dependence of the phase reflection coefficient (ϕ_2) on the permittivity of the dielectric layer, as discussed below. We will focus on deriving the mathematical model for ϕ_2; ϕ_1 can be determined using a full-wave simulation.

In our previous work [41], the phase reflection coefficient of the open end was derived as:

$$\phi_2 = -2\tan^{-1}(2\pi f Z_0 C) \tag{2}$$

where f is the frequency of the microwave signal; Z_0 is the characteristic impedance of the coaxial cable; and, C is the static capacitance at the open end that contains the fringing electric field. C is given by [42]:

$$C = \varepsilon_r \left\{ \frac{2\varepsilon_0}{[\ln(b/a)^2]} \int_a^b \int_a^b \int_0^\pi \frac{\cos\phi' d\rho d\rho' d\phi'}{\sqrt{[\rho^2 + \rho'^2 - 2\rho\rho'\cos\phi']}} + \frac{4\varepsilon_0}{[\ln(b/a)^2]} \sum_{n=1}^{\infty} \int_a^b \int_a^b \int_0^\pi \frac{\cos\phi' d\rho d\rho' d\phi'}{\sqrt{[\rho^2 + \rho'^2 + 4n^2d^2 - 2\rho\rho'\cos\phi']}} \right\} \tag{3}$$

where ρ and ρ´ denote the radial direction, and ϕ' denotes the azimuthal direction; a and b are the radii of the inner and outer conductors of the coaxial cable; ε_0 is the permittivity of vacuum; ε_r is the relative permittivity of the material in the gap; and, d is the gap distance between the open end of the coaxial cable and the porous metal plate. We demonstrated that for a given dielectric material, e.g., air ($\varepsilon_r = 1$), the static capacitance increases exponentially as the thickness of the air dielectric layer d decreases, resulting in the resonance frequency of the OE-HCCR decreasing exponentially [41]. Examining Eq. (3), one realizes that for a given thickness d, the static capacitance C is linearly proportional to the relative permittivity of the dielectric layer. Therefore, Eq. (3) can be simplified as:

$$C = \psi(d)\cdot\varepsilon_r \tag{4}$$

where ψ(d) corresponds to the part of the equation inside the braces in Eq. (3), indicating a linear relationship between the static capacitance and the relative permittivity of the dielectric layer. As discussed above, ψ(d) increases exponentially as the thickness d decreases. As the thickness of the dielectric layer d decreases, the static capacitance C is expected to have a greater dependence on the relative permittivity of the layer. Therefore, the resonance frequency will have a greater dependence on the relative permittivity of the layer. Hence, a decrease in the thickness of the dielectric layer can enhance the sensitivity of the OE-HCCR to variations of the dielectric properties of the layer in front of the open end, revealing a novel sensitivity enhancement mechanism of the OE-HCCR for chemical sensing applications. Fig. 2 presents the results of numerical investigations of the sensitivity enhancement mechanism. Fig. 2(a) shows the calculated relative shift in the fundamental resonance frequency (i.e., the shift in resonance frequency/initial resonance frequency, $\Delta f/f$) of the OE-HCCR as a function of the relative permittivity of the dielectric layer for five different settings of the thickness of the dielectric layer, d. As the thickness d decreased from 2 mm to 0.2 mm, larger negative shifts in the resonance frequency were obtained as the relative permittivity of the layer increased from 1 to 5. Nonlinear relationships were revealed as shown in Fig. 2(a). Fig. 2(b) shows the calculated dielectric measurement sensitivity of the OE-HCCR, i.e., relative frequency shift/change in relative permittivity (changing from 1 to 1.5), as a function of the thickness of the dielectric layer. The dielectric measurement sensitivity increased as the thickness of the dielectric layer decreased, as expected. Fig. 2(b) predicts the potential for developing a highly-sensitive chemical sensor based on the OE-HCCR. A proof of concept for the dielectric sensitivity enhancement can be found in our recent work [43]. The limit of detection of the prototype OE-HCCR with respect to a change in relative permittivity of the dielectric layer in the gap is estimated to be approximately 4 ppm given that a change in the resonance frequency can be resolved to 1 kHz by a state-of-the-art RF interrogator.

2.2. OE-HCCR-MOF sensor design

Based on the OE-HCCR platform, a highly-sensitive gas sensor was invented, the OE-HCCR-MOF probe. An overview of the OE-HCCR-MOF probe is presented in Fig. 3, including a schematic and a photograph of a prototype probe. Fig. 3(a) shows a schematic of the proposed gas sensor based on an OE-HCCR and a thin layer of metal-organic framework (MOF) placed within the gap volume. The thin layer of MOF powder (~200 μm thickness, commercial HKUST-1) filled the gap between the microporous metal plate and the open end of the coaxial cable. Note that the thickness of the MOF is defined by the thickness of the circular spacer (i.e., a gasket) and can be varied by using spacers with different thicknesses. In the sensor design, the thickness of the dielectric layer (MOF) was designed to be 0.2 mm because this setting offers a relatively high measurement sensitivity (see Fig. 2). Over a small dynamic range (e.g., ~0.2 change in permittivity), the relationship between the frequency shift and variations in permittivity of the dielectric layer can be considered a linear function. Fig. 3(b) shows a photograph of a prototype device. The center part of the porous metal plate was made of PM-35 permeable steel with pore sizes of 25 ± 15 μm. The OE-HCCR was used to interrogate changes in the relative permittivity of the MOF layer due to the adsorption of guest molecules from the surrounding environment. Specifically, since the MOF has a large surface-to-volume ratio and most of the MOF's volume consists of open pores, adsorption of guest molecules from the surrounding environment into these open pores will increase the relative permittivity of the guest-loaded MOF layer. Consequently, the responses from all of the empty or filled pores are summed to produce permittivity changes by the entire guest-loaded MOF layer. The change in the relative permittivity of the MOF layer results in the variation of the total capacitance at the open end, leading to a change in the phase reflection coefficient associated with the open end. The change in the phase reflection coefficient at the open end will change the phase-matching condition of the microwave cavity resonator and thereby shift the resonance frequency. Therefore, by tracking the shift of the resonance frequency, the overall change in the relative permittivity of the MOF layer can be monitored in real-time. In other words, the changes in the overall relative permittivity of the MOF layer, induced by the loading and unloading of guest molecules within the porous structure can, in turn, be employed to measure the temporal process of guest adsorption and desorption. Furthermore, it is possible to determine the concentration of the guests in the host (after sensor calibration) at any time by simply tracking the resonance frequency shift of the microwave cavity resonator.

2.3. Material

The MOF used in the prototype device was HKUST-1, purchased from ACS Material LLC (Pasadena CA, USA). The MOF was prepared by a hydrothermal method and yielded particles ranging in size from 10 to 20 μm. The MOF pore size was approximately 0.6 nm. The tapped density of the MOF powder was ~0.45 g/mL. Fig. 4 contains

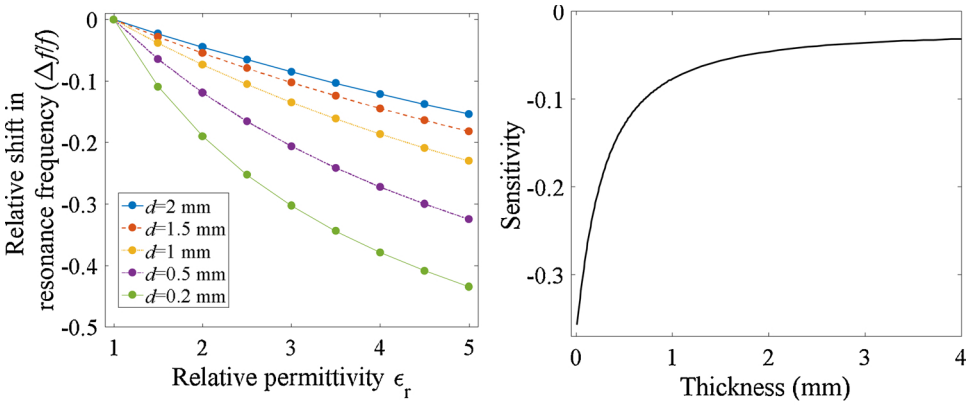

Fig. 2. Numerical investigations of the OE-HCCR for chemical sensing with enhanced sensitivity. (a) The relative shift in the resonance frequency of the OE-HCCR as a function of the relative permittivity of the dielectric layer for five different values of the layer thickness (2, 1.5, 1, 0.5, and 0.2 mm). (b) The dielectric measurement sensitivity of the OE-HCCR as a function of the thickness of the dielectric layer. The measurement sensitivity is obtained by differentiating the relative frequency shift with respect to the change in the relative permittivity of the dielectric layer (increment of 0.5, increasing from 1 to 1.5).

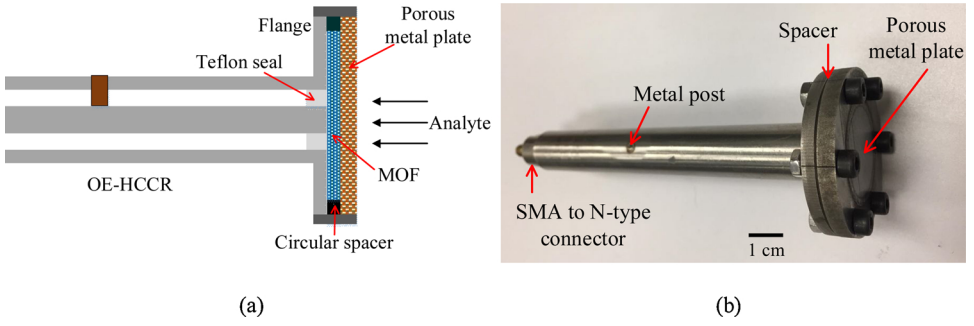

Fig. 3. The OE-HCCR-MOF gas sensor. (a) A schematic of the probe. The thickness of the MOF layer is defined by the thickness of the circular spacer (i.e., a gasket), which can be varied by using spacers with different thicknesses. A porous metal plate was used to back the MOF layer and allow the gas analyte to enter into the MOF layer. (b) A photograph of a prototype probe. The prototype OE-HCCR-MOF probe was fabricated using a homemade hollow coaxial cable made of stainless steel, which can be connected to a commercial 50-Ω coaxial cable using an SMA to N-type connector.

characterization information of the MOF powder obtained from ACS Material LLC [44], including an SEM image and X-Ray diffraction (XRD) analysis results. Discrete intensive diffraction peaks at 200, 220, 222, 400, etc., were observed in the XRD spectra. The XRD spectra were measured with Cu Kα radiation. HKUST-1 was chosen for our proof-of-concept demonstration because it has well-known physical and chemical properties (e.g., CO_2 selectivity), and is commercially available. It is also a well-behaved dielectric material such that variations of the dielectric property due to loading and unloading of guest molecules can be interrogated using the microwave probe.

2.4. Experimental setup

The experimental setup for demonstrating the gas sensing capability of the prototype OE-HCCR-MOF device is illustrated in Fig. 5. The OE-HCCR-MOF sensor was connected to a vector network analyzer (VNA, Agilent 8753ES) via a communication coaxial cable through the vacuum tubing as shown in Fig. 5. The sensor was placed in a vacuum drying box where the ambient atmosphere (0.1–1.0, ± 0.1 atm) and the temperature (290–500, ± 3 K) could be controlled by built-in heating and cooling accessories. A vacuum pressure gauge was also connected to the vacuum drying box to measure the pressure. The exit port of the vacuum drying box was connected to a home-built manifold, through which the box could be evacuated using a vacuum pump (EasyVac-7, ACROSS INTERNATIONAL) and gases of interest (e.g., CO_2 and CH_4) could be injected into the box for adsorption studies.

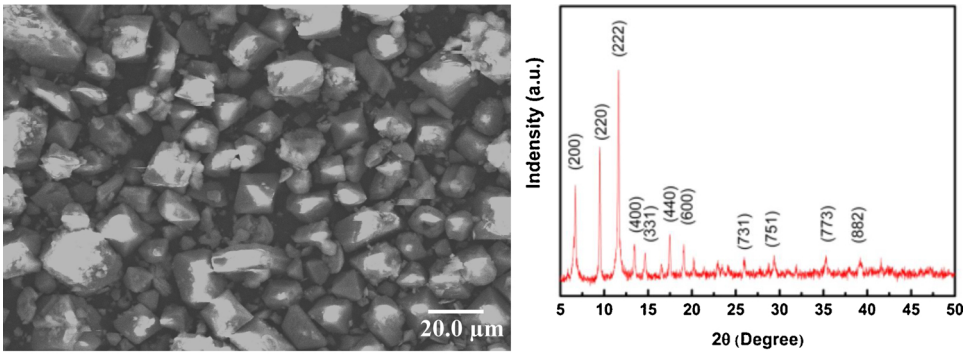

Fig. 4. Characterization of HKUST-1 MOF powder sourced from ACS Material LLC. (a) An SEM image of the commercial HKUST-1. (b) XRD spectra of the commercial HKUST-1 [44].

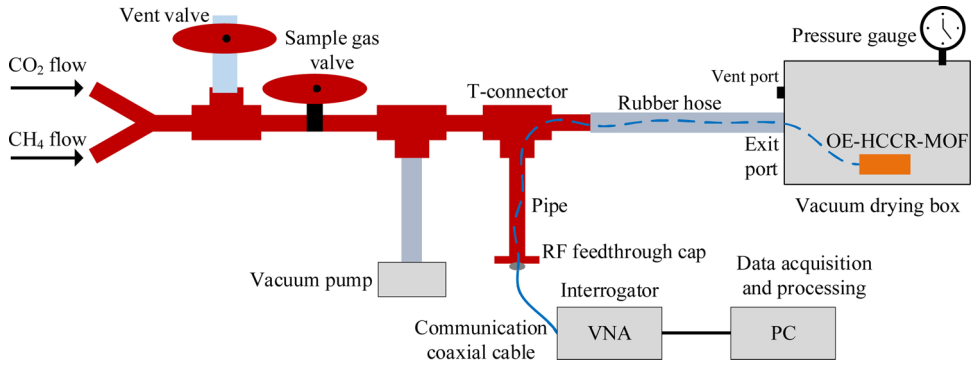

Fig. 5. Schematic of the experimental setup employed for gas adsorption tests using the OE-HCCR-MOF sensor. The OE-HCCR-MOF sensor was tested in a vacuum drying box where the composition of the gas atmosphere and the temperature was controlled.

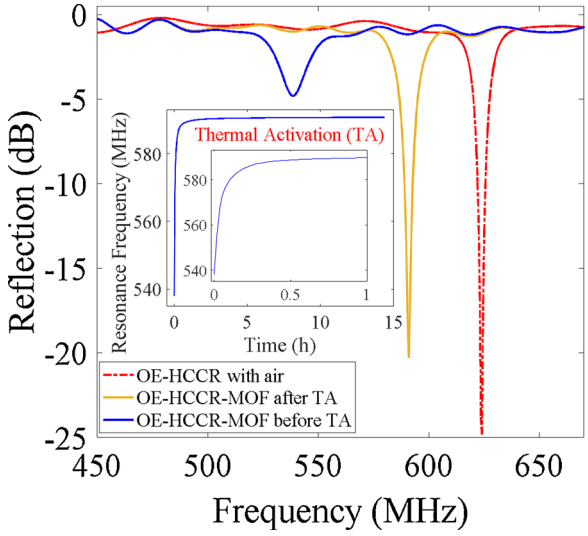

Fig. 6. Reflection spectra in the region of the fundamental resonance frequency for the prototype OE-HCCR-MOF sensor device under different conditions of the MOF layer dielectric. The red-dashed curve represents the reflection spectrum of the prototype device *before* the MOF layer was filled in the gap between the open end and the metal plate, i.e., the gap was filled with a layer of air dielectric. The solid blue and yellow curves represent the reflection spectra of the prototype device with a layer of MOF filled in the gap before and after the thermal activation (TA) process, respectively. The inset shows the evolution of the resonance frequency of the OE-HCCR-MOF sensor during the overnight TA process; an expanded view of the first hour of the TA process is also shown. (For interpretation of the references to colour in this figure legend, the reader is referred to the web version of this article).

3. Results

A series of reflection spectra near the fundamental resonance frequency for the prototype sensor device is shown in Fig. 6. The red-dashed curve represents the reflection spectrum of the prototype device before the gap between the open end and the metal plate was filled with the MOF layer, i.e., the gap was filled with a layer of air dielectric; the solid blue and yellow curves correspond to the reflection spectra of the prototype OE-HCCR-MOF device before and after thermal activation (TA) of the MOF layer, respectively. After the air gap between the open end and the metal plate was filled with a MOF layer, the resonance frequency (i.e., the dip in the reflection spectrum) of the device shifted to the lower frequency region, as expected, since the MOF has a larger relative permittivity ($\varepsilon_r \sim 2$) compared to air ($\varepsilon_r \sim 1$) in the interrogation frequency regime. After thermal activation of the MOF, the resonance frequency of the device shifted to a higher frequency. This observation is reasonable because the evacuation of the adsorbed molecules (e.g., H_2O, CO_2) in the interior MOF volume during TA resulted in a decrease in the relative permittivity of the MOF layer. The quality-factor (Q-factor) of the reflection spectrum decreased greatly as the gap between the open end and the metal plate was filled with the MOF layer (before TA). After TA, the Q-factor increased, indicating that the MOF became less lossy to the microwave signal since the polarizable water molecules were evacuated. The inset in Fig. 6 shows the continuously-monitored evolution of the resonance frequency of the OE-HCCR-MOF device during the overnight TA process; an expanded view of the first hour of the TA process is also shown. The resonance frequency of the OE-HCCR-MOF sensor device stabilized at approximately 592 MHz after TA. The resonance frequency of the OE-HCCR with air filling the gap between the open end and the metal plate was found to be 624 MHz, which differed from the calculated frequency of 636 MHz. This discrepancy is primarily due to the Teflon seal in the prototype device, which was not considered in the calculation. After TA, the OE-HCCR-MOF resonated at 592 MHz, indicating that a decrease of 32 MHz in resonance frequency was observed as the dielectric changed from air to the MOF. According to numerical calculations, the effective relative permittivity of the dehydrated HKUST-1 layer was estimated to be ~1.29 at ~590 MHz. The effective relative permittivity of the hydrated HKUST-1 layer (i.e., the MOF layer before TA) was estimated to be ~1.76 at ~550 MHz.

The detection of CO_2 gas using the OE-HCCR-MOF sensor was first demonstrated at room temperature (~23 °C). In the experiment, the box was first evacuated until the reflection spectrum of the sensor stabilized, indicating that the MOF layer was fully activated. Then the box was backfilled with pure CO_2 gas to reach the desired pressure inside the vacuum box for the adsorption test. The reflection spectrum was monitored *in situ* and data processing was performed to determine the response of the OE-HCCR-MOF sensor (i.e., resonance frequency shift) in real-time. Each measurement took approximately 3 s for the interrogation and data-processing. After the sensor stabilized (no frequency shift), the box was evacuated again and another volume of CO_2 was allowed to flow into the box (i.e., at another pressure setting), followed by a re-measurement. The experimental results for the CO_2 adsorption tests are presented in Fig. 7. Fig. 7(a) shows the absolute value of the measured resonance frequency shift (Δf) as a function of time for five different settings of CO_2 pressure inside the hermetically-sealed vacuum drying box. The evolution of the resonance frequency revealed a strong dependence of the relative permittivity of the MOF layer on the concentration of CO_2 in the surrounding atmosphere. After approximately four minutes, the resonance frequency of the sensor no longer shifted, revealing an equilibrium state of the guest/host system (CO_2@MOF). Fig. 7(b) shows the shift in the resonance frequency (Δf) as a function of CO_2 pressure at steady-state conditions. Higher pressures of CO_2 (i.e., higher concentrations) in the vacuum drying box resulted in larger frequency shifts, consistent with larger increases in the relative permittivity of the MOF layer due to the adsorption of CO_2.

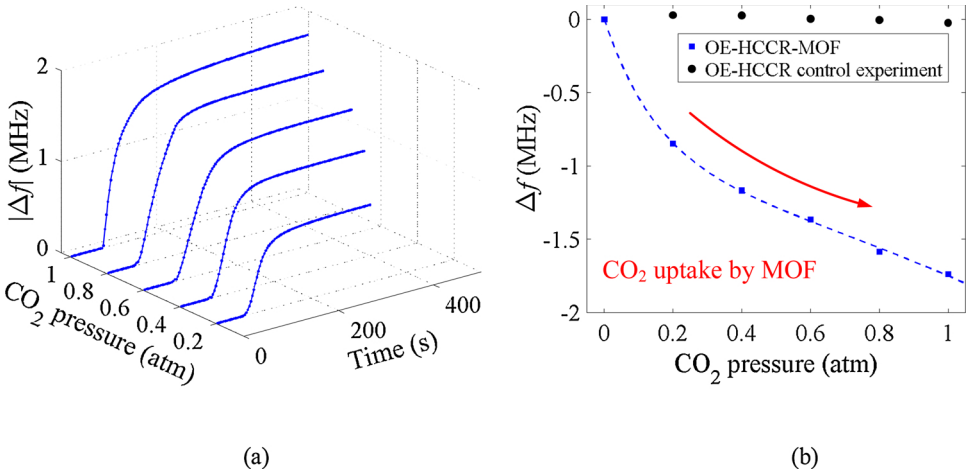

Fig. 7. Adsorption tests of CO_2 by HKUST-1 using the OE-HCCR-MOF sensor at room temperature (23 °C). (a) The evolution of the resonance frequency of the sensor for different CO_2 pressures in the vacuum drying box. (b) The resonance frequency shift (Δf) of the OE-HCCR-MOF sensor at steady-state conditions as a function of the CO_2 pressure in the box (blue solid squares). The frequency decreased by ~1.74 MHz overall for the pressure range 0-1.0 atm of the CO_2 gas atmosphere. The responses of the OE-HCCR (without the MOF layer in the gap between the metal plate and the open end) were also included as a control experiment, showing a frequency shift of approximately 0.050 MHz as the CO_2 pressure increased from 0 to 1.0 atm (black solid circles). The blue-dashed curve is fitted using an exponential model and included to guide the eye. (For interpretation of the references to colour in this figure legend, the reader is referred to the web version of this article).

Given the probe resonated at ~592 MHz, the averaged sensitivity, i.e., relative resonance frequency shift vs. change in pressure, was determined to be approximately -0.003/atm. The effective relative permittivity of the MOF layer after adsorption of CO_2 at a pressure setting of 1 atm increased by approximately 0.012. Note that the response curve of the OE-HCCR (i.e., without the MOF layer in the gap between the open end and the metal plate) was also included as a control experiment in Fig. 7(b) for comparison. The resonance frequency shifted by approximately 0.050 MHz as the pressure of CO_2 increased from 0 to 1.0 atm, which only accounted for 3% of the response of the OE-HCCR-MOF device (the case where the MOF layer was included). Therefore, the use of the MOF layer improved the gas sensing sensitivity of the OE-HCCR for CO_2. The experimental results demonstrated that the prototype OE-HCCR-MOF device could be employed for highly-sensitive and quantitative detection of CO_2 after proper calibration. Note that the measurement sensitivity of the OE-HCCR-MOF sensor also relies on the adsorption capacity of the MOF material, the higher the adsorption capacity, the larger the sensitivity [32]. The CO_2 sensitivity of the prototype OE-HCCR-MOF sensor was comparable to the CO_2 sensitivity reported in [32] where a microwave active-resonator and MOF-199-M2 were used.

The reproducibility of the OE-HCCR-MOF sensor was demonstrated by repeating the evacuation/backfill process using CO_2 gas. CO_2 gas was injected into the vacuum drying box until the pressure reached 1.0 atm, followed by evacuation after an equilibrium state was reached. Fig. 8 shows the resonance frequency shift (Δf) as a function of time during the test. The OE-HCCR-MOF device exhibited completely reversible and fast response times for adsorption/desorption of CO_2. The resonance frequency of the sensor decreased as CO_2 was injected into the vacuum drying box and plateaued after approximately four minutes, indicating that equilibrium was reached in the system. The resonance frequency increased as the vacuum drying box was evacuated due to the removal of the CO_2 adsorbed in the pores of the MOF. After the vacuum drying box was evacuated for approximately ten minutes, the resonance frequency returned to the initial value, indicating that all of the adsorped CO_2 was removed from the pores. The four-cycle evacuation/backfill test demonstrated good signal reproducibility by the prototype OE-HCCR-MOF sensor device. Note that the response time of the probe device for CO_2 adsorption is expected to be faster than the time shown in Fig. 8 (~a few minutes) because the volume of the vacuum drying box used in the experiment was large and additional time was required for the CO_2 pressure to reach 1.0 atm in the box.

Further experiments were performed to demonstrate the selectivity of the prototype OE-HCCR-MOF probe when utilized for gas sensing.

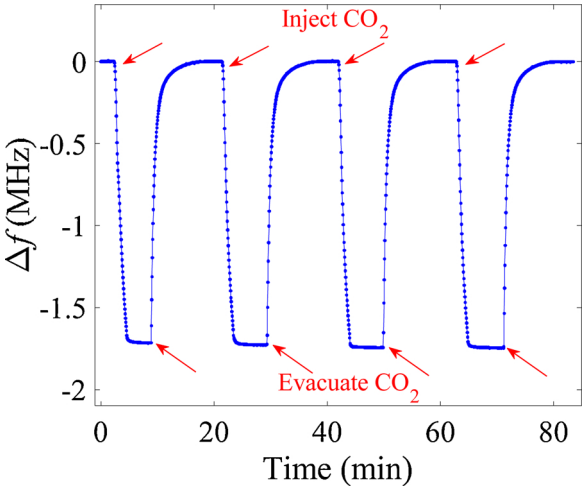

Fig. 8. Signal reproducibility test of the OE-HCCR-MOF sensor for adsorption of CO_2 by HKUST-1. CO_2 gas was injected into the vacuum drying box until the pressure reached 1.0 atm, followed by the evacuation of the gas after an equilibrium state was reached. The OE-HCCR-MOF device exhibited completely reversible and fast response times for the adsorption/desorption of CO_2 by the MOF throughout the four-cycle evacuation/backfill test.

Since it was previously reported that HKUST-1 has a differential CO_2/CH_4 selectivity, with a greater adsorption propensity for CO_2 [45], both gases were employed as the guest molecules to demonstrate the capability of the prototype OE-HCCR-MOF gas sensor for competitive chemical selectivity. In a competitive gas adsorption experiment, the vacuum drying box was first evacuated to avoid interferences caused by other vapors (e.g., humidified air) and then continuous flows of pure CH_4 and pure CO_2 gases were alternately directed into the box. The vent port was kept open to maintain the pressure in the box at 1.0 atm. For each gas (CH_4 or CO_2), the equilibrium state of the guest-loaded MOF was reached before switching to the flow of the other gas. Fig. 9 shows the recorded temporal evolution of the resonance frequency shift (Δf) during the competitive gas adsorption demonstration test. When CH_4 gas first directed into the box, the resonance frequency of the device decreased due to the adsorption of CH_4 molecules in the pores of the MOF and then plateaued, as expected. The injection of CO_2 gas resulted in further decreases in the resonance frequency. The decreasing trend of the resonance frequency was reasonable since the HKUST-1 layer has a larger adsorption propensity for CO_2 compared to CH_4 and CO_2 gas adsorption by the MOF layer causes a larger frequency shift. An

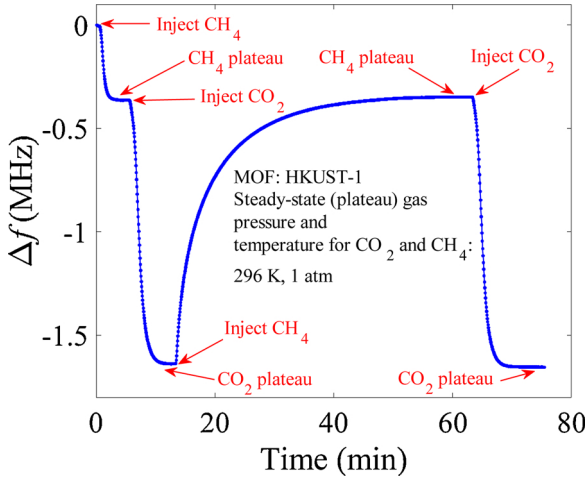

Fig. 9. A demonstration test of the competitive gas adsorption between CH_4 and CO_2 in HKUST-1. The evolution of the resonance frequency of the OE-HCCR-MOF sensor when CH_4 and CO_2 were alternately directed into the vacuum drying box, bathing the MOF dielectric. For each gas, the equilibrium state (plateau) was reached before switching to the other gas. Both the magnitudes of the frequency shifts and the time responses demonstrated that the MOF layer exhibited a larger adsorption propensity for CO_2 compared to CH_4.

increase in the density of diamagnetic guests and the consequent change in the relative permittivity of the MOF layer were expected to occur when CO_2 replaced CH_4. After the sensor stabilized in a 100 % CO_2 environment, the input gas was switched to CH_4. As CH_4 replaced CO_2 in the pores of the MOF layer (due to the large excess of CH_4 in the vacuum drying box), the relative permittivity of the MOF layer decreased due to the smaller adsorption propensity by the MOF for CH_4, increasing the resonance frequency. We found that less than 10 min were required for CO_2 to replace CH_4 in the pores of the MOF layer; conversely, approximately 50 min were required for CH_4 to replace CO_2 in the MOF pores. The time response verified that the MOF powder (HKUST-1) in the OE−HCCR-MOF sensor had a larger adsorption propensity for CO_2, which matched well with previous studies [45].

4. Discussions

The present work demonstrated a novel chemical sensor platform, the open-ended coaxial cable resonator (OE-HCCR). With the coupling of the OE-HCCR to a microporous MOF-crystal layer, a new gas sensor probe, the OE-HCCR-MOF, was formed. The MOF-crystal layer used in the demonstration was the commercially available HKUST-1 MOF. The OE-HCCR-MOF probe is a sensitive, low-cost, easy-to-fabricate, user-configurable, robust, and portable chemical sensor with quantitative chemical selectivity and real-time monitoring capability. Different dielectric MOFs targeting specific analytes can be easily integrated into the sensor platform, offering a universal strategy for chemical sensing applications. Currently, the interrogator unit for the device used in the demonstration is a benchtop VNA. However, there are various portable VNAs (e.g., Anritsu MS46121B) that also offer good performance. Alternatively, a positive feedback system can be built to interrogate the OE-HCCR-MOF probe to further decrease the size and the system cost of the interrogation unit [46]. The proposed OE-HCCR is essentially a scientific advancement of the well-known open-ended coaxial probes. By fabricating a resonating structure from an all-metal hollow coaxial cable, the resultant OE-HCCR provides additional advantages, including ease of signal processing, improved dielectric sensitivity, and enhanced mechanical robustness. The proposed OE-HCCR provides a novel route for developing a new generation of coaxial cable-based gas sensors. Compared to other microwave gas sensors, e.g., planar ring resonators [47], cavity resonators [48], and capacitive resonators [49], the OE-HCCR is featured in a ruggedized all-metal structure, which makes it a portable device and suitable for sensing applications in elevated-temperature harsh environments. Note that the prototype OE-HCCR shown in this work is relatively bulky. The size dimensions of the hollow coaxial cable (i.e., the diameters of the inner and outer conductors) can be further reduced based on transmission line theory. The distance between the metal post and the open end of the coaxial cable (L) can be reduced to the mm-scale. The reduction in the size dimensions of the OE-HCCR will increase the operating frequency. On the other hand, the operating frequency can also be tuned by adjusting the initial gap distance between the open end of the coaxial cable and the porous metal plate [41].

It is well known that some MOFs, e.g., HKUST-1, can strongly adsorb water molecules from the ambient environment and that the adsorbed water molecules will block the specific affinity of the MOFs for CO_2 molecules [50]. The presence of N_2, O_2, or dry air will not interfere with the detection of the analyte of interest, e.g., CO_2. The porous structure of HKUST-1 could change irreversibly, i.e., collapse, due to water absorption, degrading the performance of the MOF-based sensor probe. In fact, in our investigations, an OE-HCCR-MOF prototype device with HKUST-1 as the MOF layer was exposed to open-air conditions for nine months. The sensing performance was then tested by investigating the sensor response to CO_2. The device exhibited an approximately 1 MHz shift in the resonance frequency as the CO_2 pressure increased from 0 to 1.0 atm. The measured frequency shift, i.e., 1 MHz, was ~ 57 % of the frequency shift for the device shown in Fig. 7, where a fresh MOF layer dielectric was employed. The decrease in the magnitude of the frequency shift indicated reduced adsorption of CO_2. We postulate that the main reason for the diminished change in the frequency shift upon CO_2 adsorption was due to the collapse or other modifications of the porous structure in the MOF because of water adsorption from the ambient environment. Therefore, additional protection of the sensor probe should be considered in order to prevent humidity from interfering and degrading the probe's sensing capability. For instance, a layer of regenerable desiccant can be coated on the outside surface of the porous metal plate so that the water molecules could be adsorbed by the desiccant layer [51] and the water-free gaseous analyte could then enter the MOF layer. Furthermore, the temperature crosstalk should be investigated since the OE-HCCR-MOF device essentially functions based on the principles of dielectric spectroscopy, and temperature variations could change the dielectric property of the MOF layer. We envision that a differential method can be employed by using a reference resonator for temperature compensation [52]. Further studies and optimizations of the OE-HCCR-MOF device are underway.

5. Conclusion

We have invented and demonstrated a novel probe that combines a dielectric composed of a MOF layer (HKUST-1) with tailored chemical properties and a novel open ended-hollow coaxial cable resonator (OE-HCCR) for sensitive and selective chemical sensing applications. We demonstrated that the adsorption and desorption of guest molecules in the MOF host system resulted in changes to the dielectric property of the MOF layer. The variations of the dielectric property of the MOF layer can be accurately determined by monitoring shifts of the resonance frequency of the microwave resonator in real-time. In addition to a layer made of MOF powders, a MOF single-crystal can also be integrated within the active volume of the OE-HCCR. The resultant OE-HCCR-single-crystal-MOF device may provide a potential route to probe the weighted positions and orientations of guest molecules in the pores of MOF using different electric field polarizations for interrogation. The proposed OE-HCCR-MOF is essentially a new portable chemical sensor platform, and its capability for dielectric measurements could find potential applications in various chemical fields due to its high sensitivity, chemical selectivity, robustness, ease of fabrication, user-configurability, and ease of signal interrogation. The proposed OE-HCCR-MOF

structure paves the way for developing a new generation of low-cost, real-time, portable, and powerful *in situ* devices for chemical analyses. A promising application of the OE-HCCR-MOF device is the detection of VOCs for diagnosis of chronic diseases in medical applications; the OE-HCCR would virtually function as an electronic nose [53].

CRediT authorship contribution statement

Chen Zhu: Conceptualization, Methodology, Writing - original draft, Software, Validation, Investigation, Writing - review & editing. **Rex E. Gerald:** Software, Validation, Investigation, Writing - review & editing. **Yizheng Chen:** Software, Validation, Investigation, Writing - review & editing. **Jie Huang:** Conceptualization, Methodology, Software, Validation, Investigation, Writing - review & editing, Supervision, Project administration.

Declaration of Competing Interest

The authors declare that they have no known competing financial interests or personal relationships that could have appeared to influence the work reported in this paper.

Acknowledgments

Research was sponsored by the Leonard Wood Institute in cooperation with the U.S. Army Research Laboratory and was accomplished under Cooperative Agreement Number W911NF-14-2-0034. The views and conclusions contained in this document are those of the authors and should not be interpreted as representing the official policies, either expressed or implied, of the Leonard Wood Institute, the Army Research Laboratory or the U.S. Government. The U.S. Government is authorized to reproduce and distribute reprints for Government purposes notwithstanding any copyright notation hereon. We acknowledge support from the National Science Foundation under award number 2027571. We also acknowledge partial support from the Missouri University of Science and Technology Center for Biomedical Research.

References

[1] L.E. Kreno, K. Leong, O.K. Farha, M. Allendorf, R.P. Van Duyne, J.T. Hupp, Metal–organic framework materials as chemical sensors, Chem. Rev. 112 (2011) 1105–1125.
[2] A.H. Khoshaman, B. Bahreyni, Application of metal organic framework crystals for sensing of volatile organic gases, Sens. Actuators B Chem. 162 (2012) 114–119.
[3] P. Kumar, A. Deep, K.-H. Kim, Metal organic frameworks for sensing applications, Trac Trends Anal. Chem. 73 (2015) 39–53.
[4] M.H. Zarifi, P. Shariaty, Z. Hashisho, M. Daneshmand, A non-contact microwave sensor for monitoring the interaction of zeolite 13X with CO2 and CH4 in gaseous streams, Sens. Actuators B: Chem. 238 (2017) 1240–1247.
[5] M. Fayaz, M.J. Lashaki, M. Abdolrazzaghi, M.H. Zarifi, Z. Hashisho, M. Daneshmand, et al., Monitoring the residual capacity of activated carbon in an emission abatement system using a non-contact, high resolution microwave resonator sensor, Sens. Actuators B: Chem. 282 (2019) 218–224.
[6] N.R. Tanguy, B. Wiltshire, M. Arjmand, M.H. Zarifi, N. Yan, Highly sensitive and contactless ammonia detection based on nanocomposites of phosphate-functionalized reduced graphene oxide/polyaniline immobilized on microstrip resonators, ACS Appl. Mater. Interfaces 12 (2020) 9746–9754.
[7] H. Xiao, J. Zhang, J. Dong, M. Luo, R. Lee, V. Romero, Synthesis of MFI zeolite films on optical fibers for detection of chemical vapors, Opt. Lett. 30 (2005) 1270–1272.
[8] J. Zhang, X. Tang, J. Dong, T. Wei, H. Xiao, Zeolite thin film-coated long period fiber grating sensor for measuring trace organic vapors, Sens. Actuators B Chem. 135 (2009) 420–425.
[9] A. Venkatasubramanian, J.-H. Lee, R.J. Houk, M.D. Allendorf, S. Nair, P.J. Hesketh, Characterization of HKUST-1 crystals and their application to MEMS microcantilever array sensors, ECS Trans. 33 (2010) 229–238.
[10] J.R. Long, O.M. Yaghi, The pervasive chemistry of metal–organic frameworks, Chem. Soc. Rev. 38 (2009) 1213–1214.
[11] J. Lee, O.K. Farha, J. Roberts, K.A. Scheidt, S.T. Nguyen, J.T. Hupp, Metal–organic framework materials as catalysts, Chem. Soc. Rev. 38 (2009) 1450–1459.
[12] U. Mueller, M. Schubert, F. Teich, H. Puetter, K. Schierle-Arndt, J. Pastre, Metal–organic frameworks—prospective industrial applications, J. Mater. Chem. 16 (2006) 626–636.
[13] E. Udd, W.B. Spillman Jr., Fiber Optic Sensors: an Introduction for Engineers and Scientists, John Wiley & Sons, 2011.
[14] J. Huang, T. Wang, L. Hua, J. Fan, H. Xiao, M. Luo, A coaxial cable Fabry-Perot interferometer for sensing applications, Sensors 13 (2013) 15252–15260.
[15] T. Wei, S. Wu, J. Huang, H. Xiao, J. Fan, Coaxial cable bragg grating, Appl. Phys. Lett. 99 (2011) 113517.
[16] C. Zhu, Y. Chen, Y. Zhuang, J. Huang, A centimeter-range displacement sensor based on a hollow coaxial cable Fabry–Perot resonator, IEEE Sens. 18 (2018) 4436–4442.
[17] A. Urrutia, I.D. Villar, P. Zubiate, C.R. Zamarreño, A comprehensive review of optical fiber refractometers: toward a standard comparative criterion, Laser Photon. Rev. (2019) 1900094.
[18] M.A. Stuchly, S.S. Stuchly, Coaxial line reflection methods for measuring dielectric properties of biological substances at radio and microwave frequencies-A review, IEEE Trans. Instrum. Meas. 29 (1980) 176–183.
[19] C. Zhu, Y. Zhuang, Y. Chen, J. Huang, A hollow coaxial cable Fabry–Pérot resonator for liquid dielectric constant measurement, Rev. Sci. Instrum. 89 (2018) 045003.
[20] S. Zeng, A. Trontz, Z. Cao, H. Xiao, J. Dong, Characterizing the gas adsorption-dependent dielectric constant for silicalite nanoparticles at microwave frequencies by a coaxial cable Fabry-Pérot interferometric sensing method, Madridge J. Nanotechnol. Nanosci. 3 (2018) 100–107.
[21] S. Eslava, L. Zhang, S. Esconjauregui, J. Yang, K. Vanstreels, M.R. Baklanov, et al., Metal-organic framework ZIF-8 films as low-κ dielectrics in microelectronics, Chem. Mater. 25 (2012) 27–33.
[22] G. Lu, J.T. Hupp, Metal− organic frameworks as sensors: a ZIF-8 based Fabry− Pérot device as a selective sensor for chemical vapors and gases, J. Am. Chem. Soc. 132 (2010) 7832–7833.
[23] J. Hromadka, B. Tokay, S. James, R.P. Tatam, S. Korposh, Optical fibre long period grating gas sensor modified with metal organic framework thin films, Sens. Actuators B Chem. 221 (2015) 891–899.
[24] K.-J. Kim, P. Lu, J.T. Culp, P.R. Ohodnicki, Metal–organic framework thin film coated optical fiber sensors: a novel waveguide-based chemical sensing platform, ACS Sens. 3 (2018) 386–394.
[25] X. Chong, K.-J. Kim, E. Li, Y. Zhang, P.R. Ohodnicki, C.-H. Chang, et al., Near-infrared absorption gas sensing with metal-organic framework on optical fibers, Sens. Actuators B Chem. 232 (2016) 43–51.
[26] J. Hromadka, B. Tokay, R. Correia, S.P. Morgan, S. Korposh, Highly sensitive volatile organic compounds vapour measurements using a long period grating optical fibre sensor coated with metal organic framework ZIF-8, Sens. Actuators B Chem. 260 (2018) 685–692.
[27] M. Nazari, M.A. Forouzandeh, C.M. Divarathne, F. Sidiroglou, M.R. Martinez, K. Konstas, et al., UiO-66 MOF end-face-coated optical fiber in aqueous contaminant detection, Opt. Lett. 41 (2016) 1696–1699.
[28] C. Zhu, J.A. Perman, R.E. Gerald, S. Ma, J. Huang, Chemical detection using a metal–organic framework single crystal coupled to an optical fiber, ACS Appl. Mater. Interfaces 11 (2019) 4393–4398.
[29] J. Hromadka, B. Tokay, R. Correia, S.P. Morgan, S. Korposh, Carbon dioxide measurements using long period grating optical fibre sensor coated with metal organic framework HKUST-1, Sens. Actuators B: Chem. 255 (2018) 2483–2494.
[30] E. Miliutina, O. Guselnikova, S. Chufistova, Z. Kolska, R. Elashnikov, V. Burtsev, et al., Fast and all-optical hydrogen sensor based on gold-coated optical Fiber functionalized with metal-organic framework layer, ACS Sens. (2019).
[31] K.-J. Kim, J.T. Culp, P.R. Ohodnicki, P.C. Cvetic, S. Sanguinito, A.L. Goodman, et al., Alkylamine-integrated metal–organic framework-based waveguide sensors for efficient detection of carbon dioxide from humid gas streams, ACS Appl. Mater. Interfaces 11 (2019) 33489–33496.
[32] M.H. Zarifi, A. Gholidoust, M. Abdolrazzaghi, P. Shariaty, Z. Hashisho, M. Daneshmand, Sensitivity enhancement in planar microwave active-resonator using metal organic framework for CO2 detection, Sens. Actuators B: Chem. 255 (2018) 1561–1568.
[33] C. Zhu, Y. Zhuang, Y. Chen, J. Huang, A liquid-level sensor based on a hollow coaxial cable Fabry–Perot resonator with micrometer resolution, IEEE Trans. Instrum. Meas. 67 (2018) 2892–2897.
[34] C. Zhu, Y. Zhuang, Y. Chen, B. Zhang, J. Huang, Contactless liquid interface measurement based on a hollow coaxial cable resonator, Sens. Actuators A Phys. 285 (2019) 623–627.
[35] C. Zhu, Y. Chen, Y. Zhuang, J. Huang, Displacement and strain measurement up to 1000° C using a hollow coaxial cable fabry-perot resonator, Sensors (Basel, Switzerland) 18 (2018).
[36] S. Zeng, A. Trontz, W. Zhu, H. Xiao, J. Dong, A metal-ceramic coaxial cable Fabry-Pérot microwave interferometer for monitoring fluid dielectric constant, Sens. Actuators A Phys. 257 (2017) 1–7.
[37] P. De Langhe, K. Blomme, L. Martens, D. De Zutter, Measurement of low-permittivity materials based on a spectral-domain analysis for the open-ended coaxial probe, IEEE Trans. Instrum. Meas. 42 (1993) 879–886.
[38] A. La Gioia, E. Porter, I. Merunka, A. Shahzad, S. Salahuddin, M. Jones, et al., Open-ended coaxial probe technique for dielectric measurement of biological tissues: challenges and common practices, Diagnostics 8 (2018) 40.
[39] D. Xu, L. Liu, Z. Jiang, Measurement of the dielectric properties of biological substances using an improved open-ended coaxial line resonator method, IEEE Trans. Microw. Theory Tech. 35 (1987) 1424–1428.
[40] S. Fan, D. Misra, A study on the metal-flanged open-ended coaxial line terminating in a conductor-backed dielectric layer, 7th IEEE Conference on Instrumentation and Measurement Technology, IEEE, 1990, pp. 43–46.
[41] C. Zhu, R.E. Gerald, Y. Chen, J. Huang, Probing the theoretical ultimate limit of coaxial cable sensing: measuring nanometer-scale displacements, IEEE Trans.

Microw. Theory Tech. (2019).
[42] S. Fan, K. Staebell, D. Misra, Static analysis of an open-ended coaxial line terminated by layered media, IEEE Trans. Instrum. Meas. 39 (1990) 435–437.
[43] C. Zhu, Y. Chen, R.E. Gerald, J. Huang, Highly-sensitive Open-ended Coaxial Cable-based Microwave Resonator for Humidity Sensing, to Be Submitted, (2020).
[44] https://www.acsmaterial.com/metal-organic-framework-cu-btc-hkust-1.html.
[45] L. Hamon, E. Jolimaître, G.D. Pirngruber, CO2 and CH4 separation by adsorption using Cu-BTC metal− organic framework, Ind. Eng. Chem. Res. 49 (2010) 7497–7503.
[46] J. Fu, X. Wang, T. Wei, M. Wei, Y. Shen, A cost-effective geodetic strainmeter based on dual coaxial cable Bragg gratings, Sensors 17 (2017) 842.
[47] M.H. Zarifi, M. Fayaz, J. Goldthorp, M. Abdolrazzaghi, Z. Hashisho, M. Daneshmand, Microbead-assisted high resolution microwave planar ring resonator for organic-vapor sensing, Appl. Phys. Lett. 106 (2015) 062903.
[48] H. El Matbouly, N. Boubekeur, F. Domingue, Passive microwave substrate integrated cavity resonator for humidity sensing, IEEE Trans. Microw. Theory Tech. 63 (2015) 4150–4156.
[49] A. Abdelghani, P. Bahoumina, H. Hallil, S. Bila, D. Baillargeat, K. Frigue, et al., Capacitive Microwave Resonator Printed on a Paper Substrate for CNT Based Gas Sensor, 2017 IEEE MTT-S International Microwave Symposium (IMS), IEEE, 2017, pp. 513–516.
[50] N. Nijem, K. Fürsich, S.T. Kelly, C. Swain, S.R. Leone, M.K. Gilles, HKUST-1 thin film layer-by-layer liquid phase epitaxial growth: film properties and stability dependence on layer number, Cryst. Growth Des. 15 (2015) 2948–2957.
[51] S. Tao, L. Xu, J.C. Fanguy, Optical fiber ammonia sensing probes using reagent immobilized porous silica coating as transducers, Sens. Actuators B: Chem. 115 (2006) 158–163.
[52] P. Bahoumina, H. Hallil, J.-L. Lachaud, A. Abdelghani, K. Frigui, S. Bila, et al., Microwave flexible gas sensor based on polymer multi wall carbon nanotubes sensitive layer, Sens. Actuators B: Chem. 249 (2017) 708–714.
[53] F. Röck, N. Barsan, U. Weimar, Electronic nose: current status and future trends, Chem. Rev. 108 (2008) 705–725.

Chen Zhu received his B.E. degree in opto-electronics information engineering from Huazhong University of Science and Technology, Wuhan, China, in 2015. He is currently pursuing a Ph.D. degree at Missouri University of Science and Technology, Missouri, USA. His research interest is focused on the development of optical fiber and coaxial cable-based devices for sensing applications in harsh environments. He was a recipient of the IEEE Instrumentation and Measurement Society Graduate Fellowship Award from 2018 to 2019. He is a student member of OSA, SPIE, IEEE, the IEEE Instrumentation and Measurement Society, and the IEEE Microwave Theory and Techniques Society.

Rex E. Gerald II is a Research Professor in the Lightwave Technology Laboratory of the Department of Electrical and Computer Engineering at Missouri University of Science and Technology (MS&T). He received a B.A. in chemistry from the University of Chicago (UC) and a conjoint Ph.D. in physical chemistry from the University of Illinois, Chicago (UIC) and the Max Planck Institute (MPI), Heidelberg. He holds 26 US patents and co-authored more than 50 publications from research investigations conducted at UC, UIC, MPI, Argonne National Laboratory, and MS&T.

Yizheng Chen received his B.S. degree and master's degree in civil engineering from Tongji University, Shanghai, China, in 2009 and 2011, respectively. He received his Ph.D. degree in civil engineering from Missouri University of Science and Technology, Missouri, USA, in 2017. His research interest is focused on optical fiber corrosion sensors.

Jie Huang is the director of the Lightwave Technology Laboratory and assistant professor of Electrical and Computer Engineering at Missouri S&T. Dr. Huang has performed research in instrumentation and measurement for more than 10 years. Dr. Huang's research focuses on the development of optical and microwave sensors and instrumentation for applications in energy, intelligent infrastructures, clean-environment, and biomedical sensing. Dr. Huang authored or co-authored over 75 refereed articles, 60 conference papers, 1 book chapter, and 10 US patent applications (5 are issued) all in the arena of advanced sensors.